

Improving perturbation theory for open-shell molecules via self-consistency

Lan Nguyen Tran^{1,*}

¹*Ho Chi Minh City Institute of Physics, VAST, Ho Chi Minh City 700000, Vietnam*

(Dated: July 26, 2021)

We present an extension of our one-body Møller-Plesset second-order perturbation (OBMP2) method for open-shell systems. We derived the OBMP2 Hamiltonian through the canonical transformation followed by the cumulant approximation to reduce many-body operators into one-body ones. The resulted Hamiltonian consists of an uncorrelated Fock and a one-body correlation potential composing of only double excitation. Molecular orbitals and associated energy levels are then relaxed via self-consistency, similarly to Hartree-Fock, in the presence of correlation at the MP2 level. We demonstrate the OBMP2 performance by considering two examples well-known for requiring orbital optimization: bond breaking and isotropic hyperfine coupling constants. In contrast to non-iterative MP2, we show that OBMP2 can yield a smooth transition through unrestriction point and predict isotropic hyperfine coupling constants accurately.

I. INTRODUCTION

The second-order Møller-Plesset perturbation theory (MP2) performed on converged HF orbitals¹ may be the simplest correlated wavefunction method. Its accuracy depends on the quality reference wavefunctions, and it usually performs poorly for open-shell systems where unrestricted HF (UHF) orbitals are spin-contaminated notoriously^{2,3}. Moreover, the Hellmann-Feynman theorem no longer holds for non-variational method like MP2, leading to first derivative discontinuities at the unrestriction point⁴. To resolve these issues, one can perform perturbation theory on Brueckner orbitals defined such that their ground-state wavefunctions are nearly spin-pure and satisfied the Brillouin theorem⁵⁻⁷. While various Brueckner orbital methods have been proposed, their expensive costs hinder them from large-scale calculations.

Recently, orbital-optimized MP2 (OOMP2) and its spin-scaled variants have been developed actively⁸⁻¹⁰. In these methods, orbitals are optimized by minimizing the Hylleraas functional (or its generalization) with only double excitations. Therefore, they can be considered as an economical way to generate approximate Brueckner orbitals¹¹. Although OOMP2 and its variants have been shown to outperform conventional HF-based MP2 calculations for numerous properties, they still do not continuously break spin-symmetry even when there exists a broken-symmetry solution that is lower in energy¹¹. To resolve this issue, Head-Gordon and his coworkers have proposed different semi-empirical regularization schemes, including a simple level shift of the energy denominator¹¹⁻¹³ or orbital energy-dependent regularizers¹⁴.

In addition to wavefunction perturbation theories, double hybrid functionals (DHF) with a scaled correction of perturbative energy to the solution of Kohn-Sham equations have been developed actively^{15,16}. DHFs are constructed on the top of hybrid functionals by replacing part of the DFT correlation functional with a nonlocal correlation contribution based on perturbation theory. They are considered as the fifth rung of the DFT Jacob's

ladder and have been shown to outperform conventional functionals in many cases^{15,16}. For example, Kossmaan and coworkers found that the functional B2PLYP predicted hyperfine coupling constants more accurately than hybrid functionals and HF-based MP2¹⁷. However, similar to HF-based perturbation theory, DHFs also exhibit first derivative discontinuities at the unrestriction point. To resolve this artificial problem, Peverati and Head-Gordon proposed orbital-optimized DHFs (OODHFs)¹⁸.

Very recently, OOMP2 and OODHF orbitals have been used as references for coupled-cluster singles and doubles with perturbative triples [CCSD(T)]¹⁹ and the third-order Møller-Plesset perturbation theory (MP3)^{20,21}, yielding results several times more accurate than HF-based counterparts. Generally speaking, the quality of reference orbitals is one of the crucial factors for the accuracy of single-shot correlation methods. In general, low-scaling methods generating proper reference orbitals for high-level correlation methods are highly desirable.

We have developed a self-consistent perturbation theory named one-body MP2 (OBMP2)²². The central idea of OBMP2 is the use of canonical transformation²³⁻²⁸ followed by the cumulant approximation²⁹⁻³² to derive an effective one-body Hamiltonian. The resulted OBMP2 Hamiltonian is a sum of the Fock operator and a one-body correlation potential including only double excitations. At each iteration, the OBMP2 Hamiltonian, as a *correlated* Fock operator, is diagonalized to give eigenvectors and eigenvalues corresponding to molecular orbitals and orbital energies, respectively. Consequently, both numerator (related to molecular orbitals) and denominator (associated with orbital energies) of the double-excitation amplitude typical for MP2 will be updated simultaneously, resulting in a full self-consistency. One can thus expect that OBMP2 can resolve issues caused by the non-iterative nature of standard MP2 calculations.

In the current paper, we extend OBMP2 to open-shell systems. We first present the formulation of OBMP2 in spin orbitals. We then discuss its applications to two open-shell examples well-known for demanding orbital optimization: bond breaking and isotropic hyperfine coupling constants (HFCCs). In contrast to HF-based MP2,

we will show that OBMP2 can smooth out the transition from restricted to unrestricted solutions and predict isotropic HFCCs accurately. Finally, we will briefly discuss some implications for OBMP2 extension to a broad class of chemistry problems.

II. THEORY

We hereafter use the following notation for indices: $\{p, q, r, \dots\}$ refer to general spatial orbitals, $\{i, j, k, \dots\}$ to occupied spatial orbitals, $\{a, b, c, \dots\}$ to virtual spatial orbitals, and $\{\sigma, \sigma'\}$ to spin indices. Einstein's convention is used to present the summations over repeated indices. Our OBMP2 approach was derived through the canonical transformation developed by Yanai and his coworkers^{23–28}. In this approach, an effective Hamiltonian that includes dynamic correlation effects is achieved by a similarity transformation of the molecular Hamiltonian \hat{H} using a unitary operator $e^{\hat{A}}$:

$$\hat{H} = e^{\hat{A}\dagger} \hat{H} e^{\hat{A}} = \hat{H} + [\hat{H}, \hat{A}] + \frac{1}{2} [[\hat{H}, \hat{A}], \hat{A}] + \dots, \quad (1)$$

with the anti-Hermitian excited operator $\hat{A} = -\hat{A}^\dagger$, and the molecular Hamiltonian in spin orbitals as

$$\hat{H} = h_{q\sigma}^{p\sigma} \hat{a}_{p\sigma}^{q\sigma} + \frac{1}{2} g_{q\sigma s\sigma'}^{p\sigma r\sigma'} \hat{a}_{p\sigma r\sigma'}^{q\sigma s\sigma'} \quad (2)$$

The second equality line in Eq. 1 is the Baker–Campbell–Hausdorff (BCH) expansion, which is usually cut off at the second-order term. In OBMP2, the cluster operator \hat{A} is modeled such that including only double excitation

$$\hat{A} = \hat{A}_D = \frac{1}{2} T_{i\sigma j\sigma'}^{a\sigma b\sigma'} (\hat{a}_{i\sigma j\sigma'}^{a\sigma b\sigma'} - \hat{a}_{a\sigma b\sigma'}^{i\sigma j\sigma'}), \quad (3)$$

with the MP2 amplitude

$$T_{i\sigma j\sigma'}^{a\sigma b\sigma'} = \frac{g_{i\sigma j\sigma'}^{a\sigma b\sigma'}}{\epsilon_{i\sigma} + \epsilon_{j\sigma'} - \epsilon_{a\sigma} - \epsilon_{b\sigma'}}, \quad (4)$$

where $\epsilon_{i\sigma}$ is the orbital energy of the spin-orbital $i\sigma$. Substituting the operator \hat{A}_D into the canonical transformation (Eq 1), we can have an effective Hamiltonian including dynamical correlation at the level of second-order perturbation.

To derive the working equation of OBMP2 Hamiltonian, we introduced three approximations. First, we truncated the BCH expansion at the second order

$$\hat{H}_{\text{OBMP2}} = \hat{H}_{\text{HF}} + [\hat{H}, \hat{A}_D]_1 + \frac{1}{2} [[\hat{H}, \hat{A}_D], \hat{A}_D]_1. \quad (5)$$

This truncation is correct through the second order in perturbation. Second, we approximate the zeroth-order BCH expansion \hat{H} (Eq. 2) by the HF Hamiltonian \hat{H}_{HF}

$$\hat{H}_{\text{HF}} = \hat{F} + C = f_{q\sigma}^{p\sigma} \hat{a}_{p\sigma}^{q\sigma} + C \quad (6)$$

where \hat{F} is the Fock operator, $f_{q\sigma}^{p\sigma}$ and C are the Fock matrix in spin-orbital basis and a constant, respectively:

$$f_{q\sigma}^{p\sigma} = h_{q\sigma}^{p\sigma} + 2g_{q\sigma i\sigma'}^{p\sigma i\sigma'} - g_{i\sigma' q\sigma}^{p\sigma i\sigma'}, \quad (7)$$

$$C = -2g_{i\sigma j\sigma'}^{i\sigma j\sigma'} + g_{j\sigma' i\sigma}^{i\sigma j\sigma'}. \quad (8)$$

Third, we employ the cumulant approximation^{29–32} to reduce many-body operators into one-body ones (see Appendix A), and commutators with the subscription 1, $[\dots]_1$, involve one-body operators and constants only.

Substituting Eqs. 2, 3, 4, 6, and 7 into Eq. 5, we arrived at the OBMP2 Hamiltonian as follows

$$\hat{H}_{\text{OBMP2}} = \hat{H}_{\text{HF}} + \hat{V}_{\text{OBMP2}} \quad (9)$$

$$\hat{V}_{\text{OBMP2}} = C' + \hat{V} \quad (10)$$

with $\hat{V} = v_{q\sigma}^{p\sigma} \hat{a}_{p\sigma}^{q\sigma}$. Here, \hat{V} and C' consist of contributions from the first and second orders BCH expansion (Eq. 5): $\hat{V} = \hat{V}_{1^{\text{st}}\text{BCH}} + \hat{V}_{2^{\text{nd}}\text{BCH}}$ and $C' = C'_{1^{\text{st}}\text{BCH}} + C'_{2^{\text{nd}}\text{BCH}}$. Their working tensor contraction expressions are given as follows,

$$\begin{aligned} \hat{V}_{1^{\text{st}}\text{BCH}} &= 2\bar{T}_{i\sigma j\sigma'}^{a\sigma b\sigma'} \left[f_{i\sigma}^{j\sigma'} \hat{\Omega}(\hat{a}_{j\sigma'}^{b\sigma'}) + g_{a\sigma b\sigma'}^{i\sigma p\sigma'} \hat{\Omega}(\hat{a}_{j\sigma'}^{p\sigma'}) - g_{i\sigma j\sigma'}^{a\sigma q\sigma'} \hat{\Omega}(\hat{a}_{q\sigma'}^{b\sigma'}) \right] \\ C'_{1^{\text{st}}\text{BCH}} &= -4\bar{T}_{i\sigma j\sigma'}^{a\sigma b\sigma'} g_{a\sigma b\sigma'}^{i\sigma j\sigma'}, \\ \hat{V}_{2^{\text{nd}}\text{BCH}} &= 2f_{a\sigma}^{i\sigma} \bar{T}_{i\sigma j\sigma'}^{a\sigma b\sigma'} \bar{T}_{j\sigma' k\sigma}^{b\sigma' c\sigma} \hat{\Omega}(\hat{a}_{c\sigma}^{k\sigma}) + f_{c\sigma}^{a\sigma} T_{i\sigma j\sigma'}^{a\sigma b\sigma'} \bar{T}_{i\sigma l\sigma'}^{c\sigma b\sigma'} \hat{\Omega}(\hat{a}_{l\sigma'}^{i\sigma'}) + f_{c\sigma}^{a\sigma} T_{i\sigma j\sigma'}^{a\sigma b\sigma'} \bar{T}_{k\sigma j\sigma'}^{c\sigma b\sigma'} \hat{\Omega}(\hat{a}_{i\sigma}^{k\sigma}) \\ &\quad - f_{i\sigma}^{k\sigma} T_{i\sigma j\sigma'}^{a\sigma b\sigma'} \bar{T}_{k\sigma l\sigma'}^{a\sigma b\sigma'} \hat{\Omega}(\hat{a}_{l\sigma'}^{j\sigma'}) - f_{i\sigma}^{p\sigma} T_{i\sigma j\sigma'}^{a\sigma b\sigma'} \bar{T}_{k\sigma j\sigma'}^{a\sigma b\sigma'} \hat{\Omega}(\hat{a}_{k\sigma}^{p\sigma}) + f_{i\sigma}^{k\sigma} T_{i\sigma j\sigma'}^{a\sigma b\sigma'} \bar{T}_{k\sigma j\sigma'}^{a\sigma d\sigma'} \hat{\Omega}(\hat{a}_{b\sigma}^{d\sigma'}) \\ &\quad + f_{k\sigma}^{i\sigma} T_{i\sigma j\sigma'}^{a\sigma b\sigma'} \bar{T}_{k\sigma j\sigma'}^{c\sigma b\sigma'} \hat{\Omega}(\hat{a}_{a\sigma}^{c\sigma}) - f_{c\sigma}^{a\sigma} T_{i\sigma j\sigma'}^{a\sigma b\sigma'} \bar{T}_{i\sigma j\sigma'}^{c\sigma d\sigma'} \hat{\Omega}(\hat{a}_{d\sigma'}^{b\sigma'}) - f_{p\sigma}^{a\sigma} T_{i\sigma j\sigma'}^{a\sigma b\sigma'} \bar{T}_{i\sigma j\sigma'}^{c\sigma b\sigma'} \hat{\Omega}(\hat{a}_{c\sigma}^{p\sigma}) \\ C'_{2^{\text{nd}}\text{BCH}} &= -4f_{a\sigma}^{c\sigma} T_{i\sigma j\sigma'}^{a\sigma b\sigma'} \bar{T}_{i\sigma j\sigma'}^{c\sigma b\sigma'} + 4f_{i\sigma}^{k\sigma} T_{i\sigma j\sigma'}^{a\sigma b\sigma'} \bar{T}_{k\sigma j\sigma}^{a\sigma b\sigma'}, \end{aligned}$$

where $\bar{T}_{i\sigma j\sigma'}^{a\sigma b\sigma'} = T_{i\sigma j\sigma'}^{a\sigma b\sigma'} - T_{j\sigma' i\sigma}^{a\sigma b\sigma'}$ and the symmetrization

operator $\hat{\Omega}(\hat{a}_{q\sigma}^{p\sigma}) = \hat{a}_{q\sigma}^{p\sigma} + \hat{a}_{p\sigma}^{q\sigma}$. At the end, we rewrite

\hat{H}_{OBMP2} (Eqs. 5 and 9) in a similar form to Eq. 6 for \hat{H}_{HF} as follows:

$$\hat{H}_{\text{OBMP2}} = \hat{\tilde{F}} + \bar{C} \quad (11)$$

with $\hat{\tilde{F}} = \bar{f}_{q\sigma}^{p\sigma} \hat{a}_{p\sigma}^{q\sigma}$. The elements $\bar{f}_{q\sigma}^{p\sigma}$ and \bar{C} are *correlated* analogues of the Fock matrix $f_{q\sigma}^{p\sigma}$ [Eq. 7] and C [Eq. 8] of the HF theory and are given as

$$\bar{f}_{q\sigma}^{p\sigma} = f_{q\sigma}^{p\sigma} + v_{q\sigma}^{p\sigma}, \quad (12)$$

$$\bar{C} = C + C'. \quad (13)$$

The perturbation matrix $v_{q\sigma}^{p\sigma}$ serves as the correlation potential altering the uncorrelated HF picture. The many-body effective Hamiltonian \hat{H} is replaced by the *correlated* Fock operator $\hat{\tilde{F}}$. The MO coefficients and energies can then be updated by diagonalizing the matrix \bar{f}_q^p , leading to orbital relaxation in the presence of dynamic correlation effects.

Since OBMP2 orbitals are relaxed via a full self-consistency similarly to HF, OBMP2 is satisfied the Brillouin condition: $\bar{f}_{a\sigma}^{i\sigma} = 0$. Thus, OBMP2 can be considered by definition as a variational Bruecker orbital theory. Because the OBMP2 computational cost of each iteration is the same as MP2 scaling [$O(N^5)$], it may serve as a low-cost method generating good reference orbitals for higher-level calculations. The MP2 density matrix evaluated using the double-excitation amplitude T_{ij}^{ab} ³³ is, certainly, different from the uncorrelated HF density matrix evaluated using molecular orbitals. In OBMP2, correlation is incorporated into molecular orbitals self-consistently. It is thus worth examining how different molecular properties are evaluated using HF-like and MP2-like OBMP2 density matrices. We evaluated the $\langle S^2 \rangle$ value in the same way as UHF throughout this paper. OBMP2 codes are implemented within a local version of PySCF³⁴. The next section will demonstrate OBMP2 applications to two representative open-shell examples: bond breaking and isotropic HFCCs.

III. RESULTS AND DISCUSSION

A. Bond breaking

Because the Hellmann-Feynmann theorem no longer holds for MP2, it usually shows incorrect PECs and unphysical discontinuities of first-order properties at the unrestriction point where the singularity of the inverse of the orbital Hessian matrix used for evaluating the orbital response of MP2 density matrix causes the violation of N -representability of relaxed MP2 density matrix⁴. Although approximate Brueckner orbital methods like OOMP2 and its spin-scaled variants are expected to restore the Hellman-Feynman theory and smooth out the transition through the unrestriction point, it was surprising that these methods still often show discontinuities in

PECs. Developing a stability analysis, Head-Gordon and coworkers demonstrated that for OOMP2, the restricted solution remains stable with respect to unrestricted solutions during the bond stretching, leading to a discontinuous jump in the orbitals from one stable solution to the other. To resolve this artifact, those authors have introduced different regularization schemes parameterized semi-empirically. Because OBMP2 yields orbitals considered as Bruecker orbitals through a full self-consistency, it is worth examining whether OBMP2 can smooth out the transition from restricted to unrestricted solutions.

Let us start with a single-bond breaking: LiH in cc-pVDZ. Figure 1 represents LiH potential energy curves (PEC) and the change of dipole moments with the bond length. We evaluate OBMP2 dipole moments using both HF-like and MP2-like density matrices. For comparison, we also plotted the coupled cluster singles and doubles (CCSD) dipole moment. In contrast, as seen in the left panel of Figure 1, our OBMP2 shows the smooth transition from restricted to unrestricted solutions. Both ways of OBMP2 density-matrix evaluation give dipole moments nearly identical, meaning that correlation is incorporated in molecular orbitals properly. Unlike MP2, although OBMP2 still presents a kink at the unrestriction point, it does not show any unphysical jump of dipole moment. Interestingly, the distance where the OBMP2 dipole moment starts decreasing is very close to the CCSD one.

We now consider more complicated cases C_2H_4 and C_2H_2 that have double- and triple-bond breaking, respectively. Razban *et al.* saw that the spin-opposite scaled OOMP2 (O2) method has stable restricted solutions for these two molecules, giving rise to significant discontinuities at unrestriction points¹¹. They introduced large level shifts to re-balance restricted and unrestricted solutions such that their orbitals smoothly transition between each other at the unrestriction point. Here, to see the effect of BCH truncation on orbital optimization, we present results from OBMP2 with first-order and second-order BCH truncation.

Figure 2 represents PECs and the $\langle S^2 \rangle$ value of C_2H_4 . We can see that the first-order BCH yields an incorrect PEC with a discontinuity in the unrestricted curves, corresponding to an unphysical jump of $\langle S^2 \rangle$ at the unrestriction point. The situation is somewhat similar to the unregularized O2 results observed by Razban and coworkers¹¹. In contrast, the second-order BCH exhibit PEC and $\langle S^2 \rangle$ smoothly transition through the unrestriction point, meaning that OBMP2 with the second-order BCH can rebalance restricted and unrestricted solutions without the use of any regularization. Figure 3 represents results for C_2H_2 that is even more challenging due to the triple-bond breaking. The failure of OBMP2 with the first-order BCH becomes more pronounced. While the second-order BCH exhibits a small jump of $\langle S^2 \rangle$ at the unrestriction point, it can give a smooth PEC.

In general, OBMP2 (with second-order BCH truncation) can yield continuous PECs through the unrestric-

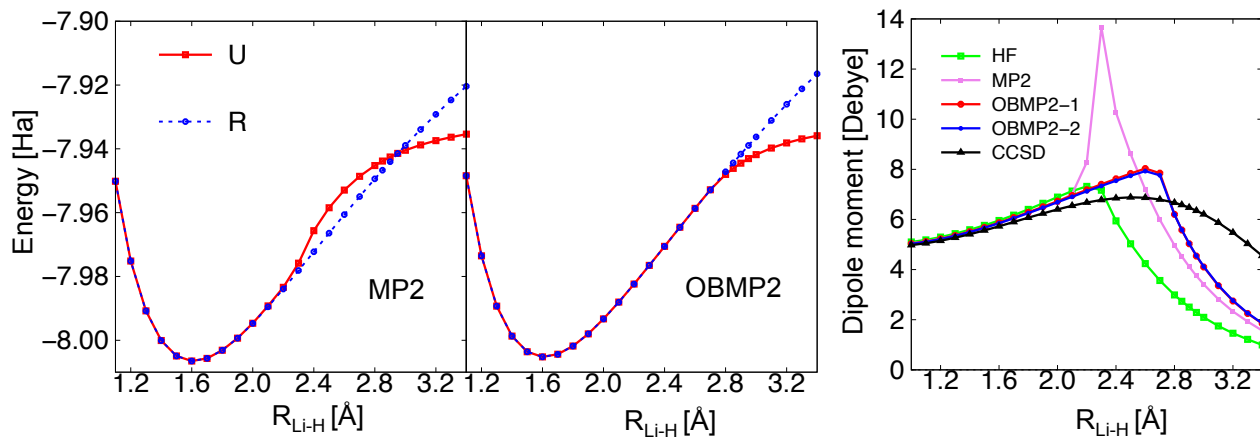


FIG. 1. Potential energy curves and dipole moments of LiH in cc-pVDZ. OBMP2 dipole moments are evaluated using HF-like (OBMP2-1) and MP2-like (OBMP2-2) density matrices.

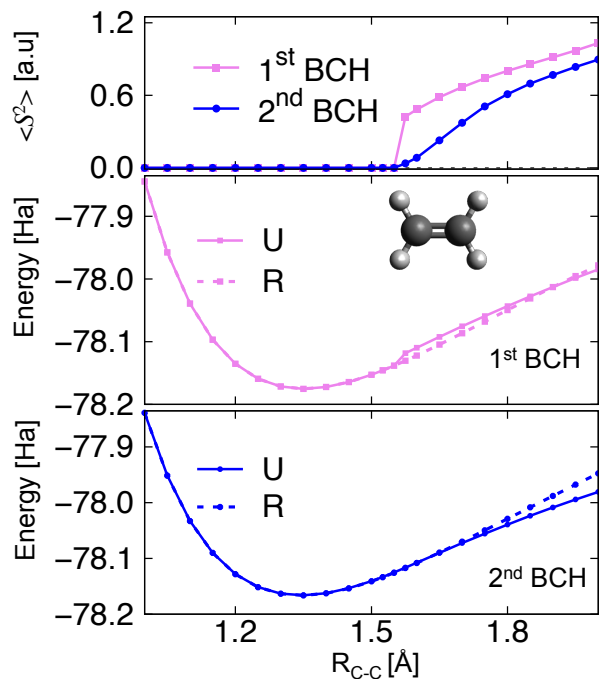


FIG. 2. Potential energy curves and $\langle S^2 \rangle$ of C_2H_4 in 6-31G from OBMP2.

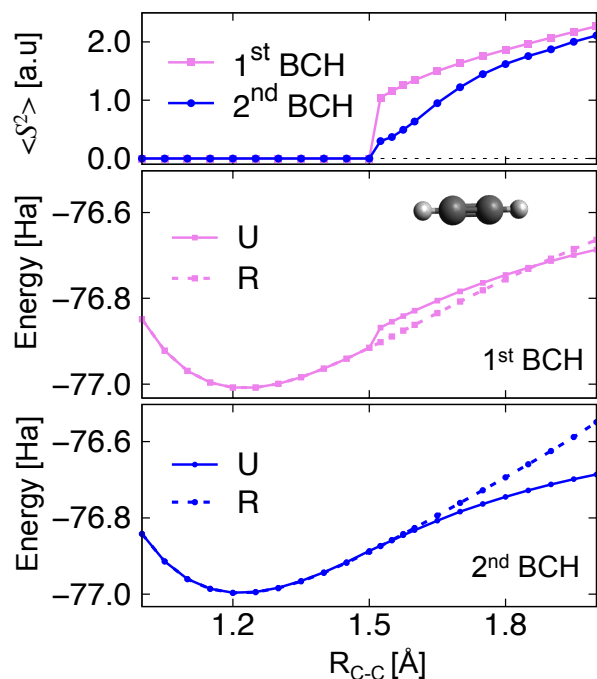


FIG. 3. Potential energy curves and $\langle S^2 \rangle$ of C_2H_2 in 6-31G from OBMP2.

tion point for molecules considered here, implying that it is promising for thermochemistry. More extensively testing it on a broader test set is thus exciting and necessary. However, it may run into issues if applying to highly challenging cases like unsymmetrical triple-bond breaking. One needs to analyze further OBMP2 solutions and employ techniques used in OOMP2 (spin-scaling and regularization) to improve the performance of OBMP2 for such cases.

B. Isotropic hyperfine-coupling constants

We now assess the performance of OBMP2 for the isotropic HFCC prediction. The isotropic HFCC describing the direct interaction between electron and nuclear spins is given by³⁵

$$A_{iso}^K = \frac{8\pi}{3} \frac{P_K}{2S} \sum_{\mu\nu} D_{\mu\nu}^{(\alpha-\beta)} \langle \chi_\mu | \delta(r_K) | \chi_\nu \rangle \quad (14)$$

where K runs over the number of nuclei; $D^{(\alpha-\beta)}$ is the spin density; P_K is the nucleus-type constant; μ and ν are atomic orbital indices; and S is the total spin. It is well-known that accurately predicting isotropic HFCCs is a highly challenging task for computational quantum chemistry. As seen in Eq. 14, the difficulty mainly arises from the direct numerical measure of spin density at nuclear positions that is sensitive to the level of electronic structure methods.

With low computational costs, DFT has been widely used for HFCC calculations. Among functionals tested, hybrid functionals like B3LYP and PBE0 were found to perform best in many cases. However, their success is sometimes attributed to fortuitous error cancellations³⁶. Some multi-configuration methods, including density matrix renormalization group (DMRG)³⁷⁻⁴⁰, complete active space second-order perturbation theory (CASPT2), and multi-reference coupled cluster (MRCC), have been assessed for HFCC prediction. Although these methods can provide accurate and reliable HFCCs, they are too expensive for large molecules. Recently, Neese and his coworkers have assessed the performance of double-hybrid functional B2PLYP and (spin-scaled) OOMP2 and found that these methods can reach accuracy comparable to CCSD(T)^{17,33}. Especially, spin-scaled OOMP2 is more accurate than the standard OOMP2. Let us now assess the performance of OBMP2 (without spin-scaling) for HFCC prediction. Here, we consider a set of 14 small doublet radicals. For comparison, we also evaluated isotropic HFCCs using MP2, two double-hybrid functions B2PLYP and DSD-PBEP86, and CCSD(T) using ORCA⁴¹. EPR-III basis set was employed, except for the elements Al and Mg for which IGLO-III and a s -decontracted TZVPP basis set were used respectively. All geometries were adopted from Ref. 42 except OH whose bond length was taken from experiment. Experimental isotropic HFCCs were adopted from Ref. 33. To see the role of orbital relaxation in OBMP2, we evaluated $D^{(\alpha-\beta)}$ using both HF-like and MP2-like ways.

First, to examine whether a method is reliable for magnetic properties, we estimate the spin contamination. In Table I, we list $\langle S^2 \rangle$ evaluated from different self-consistent methods: UHF, OBMP2, DSD-PBEP86, and B2PLYP. Note that for double-hybrid functionals, $\langle S^2 \rangle$ is evaluated only for the self-consistent DFT step, by default in ORCA. The OBMP2 $\langle S^2 \rangle$ value is evaluated in the same way as UHF. All deviations are evaluated relative to the exact $\langle S^2 \rangle$ value of doublet radicals (0.75 a.u.). UHF severely suffers from spin contamination, in particular for CO^+ and CN. Both double-hybrid functionals are less spin contaminated than UHF, and B2PLYP performs better than DSD-PBEP86. However, they both still have significant errors for CO^+ and CN. Unlike UHF, OBMP2 incorporating correlation into orbital relaxation reduces the spin contamination significantly with the smallest errors. Noticeably, it yields nearly spin-pure wavefunctions for the two most challenging cases CO^+ and CN.

TABLE I. $\langle S^2 \rangle$ values from different methods for doublet radicals. Root mean square (RMS), maximum absolute errors (MAX), and mean absolute errors (MAD) relative to the exact value (0.75).

	UHF	OBMP2	DSD-PBEP86	B2PLYP
BO	0.7999	0.7644	0.7769	0.7635
BS	0.8553	0.7747	0.8003	0.7718
CO^+	0.9825	0.7551	0.8440	0.7897
NO	0.7713	0.7551	0.7620	0.7571
AlO	0.8082	0.7596	0.7972	0.7769
CN	1.0981	0.7658	0.8701	0.7868
CH_3	0.7616	0.7560	0.7583	0.7557
H_2CO	0.7853	0.7628	0.7748	0.7662
H_2O^+	0.7579	0.7550	0.7576	0.7544
HCO	0.7656	0.7557	0.7599	0.7573
MgF	0.7505	0.7508	0.7504	0.7504
NH_2	0.7595	0.7557	0.7568	0.7551
NO_2	0.7709	0.7547	0.7636	0.7595
OH	0.7566	0.7545	0.7549	0.7538
MAX	0.3481	0.0247	0.1201	0.0397
MAD	0.0660	0.0086	0.0305	0.0142
RMS	0.1180	0.0105	0.0463	0.0186

Table II provides isotropic HFCCs from different theoretical methods and experiment. For HF-based MP2, we evaluated isotropic HFCCs using both unrelaxed and relaxed density matrices. Here, the MP2 density matrix is relaxed by solving the orbital response (coupled-perturbed HF) equation. Not surprisingly, MP2 with unrelaxed density matrices yields notoriously large errors. While MP2 with relaxed density matrices can reduce errors, they are still huge, meaning that the HF-based MP2 cannot accurately predict isotropic HFCCs. As expected, CCSD(T) can predict isotropic HFCCs well with an acceptable maximum absolute deviation (MAD). However, its maximum absolute deviation (MAX) is still large. For two DHFs, while B2PLYP yields errors similar to CCSD(T) ones, the newer functionals DSD-PBEP8 is less accurate with a huge MAX. The good performance of B2PLYP was reported previously by Neese and coworkers. Looking more closely, the errors of these methods are dominantly from Al in AlO that is well-known to be difficult for single-reference methods. The standard MP2 predicts even a wrong sign of the Al isotropic HFCC. The relaxation of MP2 density matrices via the response equation is insufficient to reach a reasonable accuracy. On the other hand, while both DHFs largely overestimate Al isotropic HFCC, CCSD(T) underestimates it. In addition to Al in AlO, C in CN is also challenging for two DHFs that underestimate their isotropic HFCC. Note that although the standard MP2 with a relaxed density matrix yields a good value for this case, the huge

TABLE II. Isotropic hyperfine coupling constant (in MHz) of small doublet radicals. Maximum (MAX) and mean absolute (MAD) deviations relative to experimental values. MP2 and OBMP2 have two isotropic HFCCs evaluated from different density matrices D . Experimental isotropic HFCCs were adopted from Ref 33.

Radicals		MP2		OBMP2		DSD-PBEP86	B2PLYP	CCSD(T)	Expt
		unrelaxed	relaxed	HF-like	MP2-like				
BO	B	1145.2	1002.5	1040.4	1034.5	1022.7	1059.7	1021.4	1033.0
	O	23.5	-78.2	-6.5	-6.7	-24.8	-14.2	-31.0	-19.0
BS	B	909.5	773.2	824.9	820.4	791.0	821.5	787.0	796.0
	S	-23.1	39.3	1.3	2.9	9.8	5.1	-1.9	-
CO ⁺	C	1901.1	1392.6	1555.6	1540.3	1480.2	1536.3	1513.9	1573.0
	O	84.7	-99.3	35.8	30.5	0.7	23.7	-38.9	19.0
NO	N	54.6	-36.9	21.8	23.0	16.7	20.9	14.8	22.0
	O	-65.2	-231.2	-30.6	-32.3	-43.3	-34.0	-48.6	-
AlO	Al	-409.7	-75.1	843.8	860.1	1217.2	973.6	573.2	766.0
	O	-53.1	128.4	17.0	9.2	64.4	21.2	9.3	2.0
CN	C	1266.1	564.5	585.5	591.8	462.0	452.5	601.8	588.0
	N	-34.2	15.3	-27.9	-20.2	-22.7	-25.6	9.6	-13.0
CH ₃	C	161.6	58.9	83.4	83.8	77.4	84.3	73.5	75.0
	H	-117.9	-71.2	-88.8	-85.5	-74.2	-69.8	-73.0	-70.0
H ₂ CO	H	236.1	282.3	316.5	316.5	297.6	325.1	298.9	372.0
	C	-134.0	-94.6	-119.3	-115.7	-97.3	-98.8	-85.6	-109.0
	O	-141.5	-42.9	-60.4	-65.8	-55.5	-57.3	-45.0	-
H ₂ O ⁺	H	-113.3	-74.0	-90.3	-88.1	-75.4	-76.8	-74.9	-73.0
	O	-146.5	-68.5	-77.4	-82.1	-79.9	-77.4	-77.0	-83.0
HCO	H	434.0	380.6	374.1	371.8	368.3	381.1	363.4	381.0
	C	373.4	340.9	382.7	379.8	375.1	387.2	366.5	377.0
	O	-64.8	-57.0	-40.8	-42.4	-40.6	-39.2	-48.7	-
MgF	Mg	-273.9	-286.6	-293.5	-292.4	-286.8	-301.6	-282.4	-337.0
	F	192.5	199.3	183.5	183.1	204.9	225.1	202.5	206.0
NH ₂	N	56.4	23.6	27.7	29.1	28.2	31.4	26.0	28.0
	H	-103.6	-64.5	-79.7	-77.1	-67.9	-66.4	-68.7	-67.0
NO ₂	N	151.2	147.7	148.3	147.5	149.8	149.0	136.7	153.0
	O	-66.5	-65.0	-62.5	-67.6	-61.0	-62.9	-60.0	-61.0
OH	O	-99.5	-40.9	-43.2	-48.7	-48.1	-54.2	-45.4	-51.0
	H	-105.1	-71.2	-84.3	-81.8	-75.1	-73.1	-73.5	-69.0
Including all cases									
	MAX	1175.7	841.1	77.8	94.1	451.2	207.6	192.8	
	MAD	127.5	67.3	16.5	16.0	37.1	24.3	23.8	
Excluding Al in AlO and C in CN									
	MAX	328.1	180.4	55.5	55.5	92.8	46.9	73.1	
	MAD	60.8	36.8	14.6	13.3	16.1	12.0	17.2	

spin contamination of the UHF reference makes this prediction unreliable. If we exclude these two challenging cases, errors of HF-based MP2 and DHFs are reduced significantly. For this analysis, while DSD-PBEP86 yields errors comparable to CCSD(T) ones, B2PLYP is even better than CCSD(T).

We now discuss our OBMP2 results. Overall, both

ways of density matrix evaluation (HF-like and MP2-like) give results close to each other with a slight deviation. We note that at the first iteration, OBMP2 isotropic HFCCs using HF-like and MP2-like density matrices are the UHF and unrelaxed MP2 values, respectively. OBMP2 can dramatically improve prediction with errors much smaller than MP2 thanks to orbital relax-

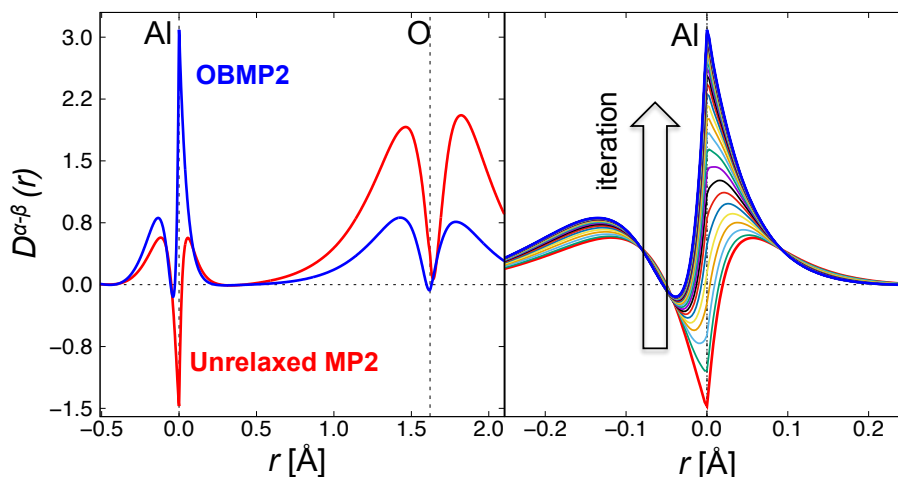


FIG. 4. One-dimensional spatial distribution of AlO spin density of the whole molecule from unrelaxed MP2 and OBMP2 (left) and around the Al center during OBMP2 iterations (right).

ation via a full self-consistency. Although it still overestimates the isotropic HFCC of Al in AlO, its errors are reasonable. Interestingly, OBMP2 is better than CCSD(T) and yields the smallest deviations. Excluding Al in AlO and C in CN changes the MADs slightly with only a few MHz, meaning that, unlike other methods, OBMP2 can treat these cases well.

Let us analyze more closely the effect of orbital optimization on isotropic HFCC prediction. Using the most challenging case AlO as an example, we plot in Figure 4 the spatial distribution of MP2-like spin density along the bond axis. In AlO, the singly occupied molecular orbital (SOMO) is characterized by a σ -bonding between Al($3s$) and O($2p_z$). Unrelaxed MP2 and OBMP2 results behave oppositely. For unrelaxed MP2, while the spin density is significantly negative at the Al center, it is largely positive around the O center, explaining why the unrelaxed MP2 gives a too negative Al isotropic HFCC. In contrast, OBMP2 reduces the spin density around the O center and yields a largely positive one at the Al center, resulting in a reasonable Al isotropic HFCC. From the right panel, we can see that the spin density at the Al center smoothly changes from negative to positive values during OBMP2 iterations, meaning that orbital relaxation in the presence of correlation is crucial for predicting the isotropic HFCCs accurately. It is important to mention that the spatial distribution of AlO spin density obtained from OBMP2 has a shape similar to that from DMRG, a much higher-level method (see Figure 2 in Ref. 37).

In general, from the benchmarking on isotropic HFCC prediction that demands the inclusion of core correlation, we see that OBMP2 is highly promising for predicting magnetic properties accurately. More extensive applications of OBMP2 to other magnetic properties are then appealing and essential.

IV. IMPLICATIONS FOR OBMP2 EXTENSION

Serving as a fully self-consistent correlated method beyond the uncorrelated HF, OBMP2 has numerous potential applications in chemistry. In addition to thermochemistry and molecular magnetic properties discussed in Section III, there exist some important possibilities of OBMP2 extension as follows:

- *Approximate Brueckner orbitals.* In OB-MP2, the correlated potential includes only double excitation, and the orbital relaxation via a full self-consistency guarantees its ground-state wavefunctions satisfied the Brillouin condition. Thus, OBMP2 is considered by definition as an approximate Brueckner orbital method alternative to high-cost Brueckner or orbital-optimized coupled cluster methods^{5,19}. Its orbitals as references to improve the accuracy of higher-level methods for open-shell molecules, such as unrestricted CCSD(T) and MP3. Also, it is interesting to examine whether OBMP2 can serve as an environment, instead of uncorrelated mean-field, in quantum embedding frameworks.
- *Excited states.* It has been shown that state-specific optimization is crucial for many excited-state problems like charge transfer and core-level excitation^{43,44}. Recently, HF-like platforms for excited-state treatment have been developed^{45,46}, and dynamic correlation via perturbation theory was incorporated non-iteratively^{45,47}. However, as we have shown here, orbital relaxation is vital for open-shell systems. Extending OBMP2 to excited states is thus appealing. One can employ techniques proposed for excited-state DFT like maximum overlap method (MOM)⁴⁸ or state-targeted energy projection (STEP)⁴⁹ to target an excited

state of interest during iterations.

- *Perturb-then-diagonalize scheme.* Multi-reference dynamic correlation methods, such as complete active space second-order perturbation theory (CASPT2), are often demanded accurate descriptions of strongly correlated systems. Unfortunately, these methods are costly and limited to small numbers of strongly correlated electrons. Alternatively, one can employ perturb-then-diagonalize methods like non-orthogonal configuration interaction in combination with MP2 (NOCI-MP2)^{50,51}, in which single HF determinants constructing Hamiltonian and overlap matrices are corrected by non-iterative MP2. It is therefore exciting to use OBMP2 determinants fully relaxed in the presence of dynamic correlation as a basis for the perturb-then-diagonalize scheme.
- *Double hybrid functionals.* Considered as the fifth rung of Jacob’s ladder, DHFs have been developed actively^{15,16}. DHFs mix a portion of correlation energy from perturbation theory, such as MP2 or random phase approximation (RPA), to hybrid exchange-correlation functionals, leading to a better performance than hybrid functionals in many cases. DHFs with orbitals optimized in the presence of all correlations were also developed, resolving some artificial issues present in DHFs with non-iterative correction¹⁸. Therefore, it will be interesting to explore new functionals employing OBMP2.

V. CONCLUSION

We have developed the unrestricted one-body MP2 (OBMP2) method for open-shell systems. The central idea is to derive an effective one-body Hamiltonian consisting of an uncorrelated Fock and a correlated potential at the MP2 level. Similar to HF counterparts, molecular orbital and orbital energies are then relaxed simultaneously by diagonalizing the correlated Fock matrix. Unlike the standard MP2, OBMP2 is thus satisfied with the Hellmann-Feynman theorem, meaning that it can bypass related challenges present in the former. Also, because OBMP2 wavefunctions fulfill the Brillouin condition, one can consider OBMP2 as a variational Brueckner orbital method.

The performance of our method has been examined using two representative open-shell examples: bond-breaking and isotropic HFCCs. Our results showed that OBMP2 dramatically outperforms standard MP2 for all cases considered here. OBMP2 can exhibit smooth potential energy curves in which restricted and unrestricted solutions coalesce at unrestricted points even for double and triple bonds in C₂H₄ and C₂H₂. It is worth noting that a systematic improvement with the order of BCH expansion was observed. Unlike orbital optimized MP2 and its variants that may need a regularization to

smooth out potential energy curves, OBMP2 with the second-order BCH does not require such a semi-empirical procedure for systems considered here. For isotropic HFCC prediction on a set of main-group doublet radicals, OBMP2 performs better than double hybrid functionals and CCSD(T), yielding the smallest errors. Plotting the change of spin density during the OBMP2 iteration, we explored the importance of orbital relaxation in the accurate isotropic HFCC prediction. Evaluating OBMP2 $\langle S^2 \rangle$ values of those doublet radicals using the same way as UHF, we saw that OBMP2 significantly reduced the spin-contamination present in UHF and provided nearly spin-pure wavefunctions. Thus, one can argue that the success of OBMP2 is not fortunate, at least for the test set considered here.

More extensive assessment is demanded to explore the performance of OBMP2 further. Like standard MP2 and OOMP2, one can use robust techniques like density-fitting or local approximations to reduce OBMP2 computational costs, making it affordable for large-size applications. As discussed in Section IV, there are many implications for extending OBMP2 to a broader class of chemistry problems. Working on these possibilities is in progress, and we hope to report on them in future works.

APPENDIX

A. One-body approximation of many-body operators

Two-body and three-body operators in the spin-orbital basis, labeled by $\{p, q, r, s, t, u\}$, are approximately written in the one-body form as,

$$\begin{aligned}
 \hat{a}_{qs}^{pr} &\Rightarrow \gamma_q^p \hat{a}_s^r + \gamma_s^r \hat{a}_q^p - \gamma_s^p \hat{a}_q^r - \gamma_q^r \hat{a}_s^p - \gamma_q^p \gamma_s^r + \gamma_s^p \gamma_q^r \\
 \hat{a}_{qsu}^{prt} &\Rightarrow (\gamma_s^r \gamma_u^t - \gamma_u^r \gamma_s^t) \hat{a}_q^p - (\gamma_q^r \gamma_u^t - \gamma_u^r \gamma_q^t) \hat{a}_s^p \\
 &\quad - (\gamma_s^r \gamma_q^t - \gamma_q^r \gamma_s^t) \hat{a}_u^p + (\gamma_q^p \gamma_u^t - \gamma_u^p \gamma_q^t) \hat{a}_s^r \\
 &\quad - (\gamma_s^p \gamma_u^t - \gamma_u^p \gamma_s^t) \hat{a}_q^r - (\gamma_q^p \gamma_s^t - \gamma_s^p \gamma_q^t) \hat{a}_u^r \\
 &\quad + (\gamma_q^p \gamma_s^r - \gamma_s^p \gamma_q^r) \hat{a}_u^t - (\gamma_u^p \gamma_s^r - \gamma_s^p \gamma_u^r) \hat{a}_q^t \\
 &\quad - (\gamma_q^p \gamma_u^r - \gamma_u^p \gamma_q^r) \hat{a}_s^t - 2 (\gamma_q^p \gamma_s^r \gamma_u^t - \gamma_s^p \gamma_q^r \gamma_u^t) \\
 &\quad - 2 (\gamma_u^p \gamma_s^r \gamma_q^t + \gamma_q^p \gamma_u^r \gamma_s^t - \gamma_s^p \gamma_u^r \gamma_q^t - \gamma_u^p \gamma_q^r \gamma_s^t)
 \end{aligned}$$

where \hat{a}_q^p , \hat{a}_{qs}^{pr} , and \hat{a}_{qsu}^{prt} are the one-, two-, and three-body second-quantized operators, respectively: $\hat{a}_q^p = \hat{a}_p^\dagger \hat{a}_q$, $\hat{a}_{qs}^{pr} = \hat{a}_p^\dagger \hat{a}_r^\dagger \hat{a}_s \hat{a}_q$, $\hat{a}_{qsu}^{prt} = \hat{a}_p^\dagger \hat{a}_r^\dagger \hat{a}_t^\dagger \hat{a}_u \hat{a}_s \hat{a}_q$. The constant γ_q^p is an element of the reduced one-body density matrix, given by

$$\gamma_q^p = \langle \Psi_0 | \hat{a}_q^p | \Psi_0 \rangle.$$

ACKNOWLEDGMENTS

This work is supported by the Vietnam Academy of Science and Technology (VAST) through the VAST Program for Young Researchers under the grant number

DLTE00.02/22-23. The author is also grateful to the HCMC Institute of Physics, VAST, for encouragement

and support. We performed all calculations on the High-Performance Computing system located at the Center for Informatics and Computing (CIC), VAST.

-
- * tnlan@hcmip.vast.vn
- ¹ Chr Møller and Milton S Plesset, "Note on an approximation treatment for many-electron systems," *Physical Review* **46**, 618 (1934).
 - ² Edward FC Byrd, C David Sherrill, and Martin Head-Gordon, "The theoretical prediction of molecular radical species: a systematic study of equilibrium geometries and harmonic vibrational frequencies," *The Journal of Physical Chemistry A* **105**, 9736 (2001).
 - ³ David Stück, Thomas A Baker, Paul Zimmerman, Westin Kurlancheek, and Martin Head-Gordon, "On the nature of electron correlation in c_{60} ," *The Journal of Chemical Physics* **135**, 11B608 (2011).
 - ⁴ Westin Kurlancheek and Martin Head-Gordon, "Violations of n -representability from spin-unrestricted orbitals in møller–plesset perturbation theory and related double-hybrid density functional theory," *Molecular Physics* **107**, 1223 (2009).
 - ⁵ Richard A Chiles and Clifford E Dykstra, "An electron pair operator approach to coupled cluster wave functions. application to he_2 , be_2 , and mg_2 and comparison with cepa methods," *The Journal of Chemical Physics* **74**, 4544 (1981).
 - ⁶ John F Stanton, Jürgen Gauss, and Rodney J Bartlett, "On the choice of orbitals for symmetry breaking problems with application to no_3 ," *The Journal of Chemical Physics* **97**, 5554 (1992).
 - ⁷ Leslie A Barnes and Roland Lindh, "Symmetry breaking in o_4^+ : an application of the brueckner coupled-cluster method," *Chemical Physics Letters* **223**, 207 (1994).
 - ⁸ Rohini C Lochan and Martin Head-Gordon, "Orbital-optimized opposite-spin scaled second-order correlation: An economical method to improve the description of open-shell molecules," *The Journal of Chemical Physics* **126**, 164101 (2007).
 - ⁹ Frank Neese, Tobias Schwabe, Simone Kossmann, Birgitta Schirmer, and Stefan Grimme, "Assessment of orbital-optimized, spin-component scaled second-order many-body perturbation theory for thermochemistry and kinetics," *Journal of Chemical Theory and Computation* **5**, 3060–3073 (2009).
 - ¹⁰ Uğur Bozkaya, Justin M Turney, Yukio Yamaguchi, Henry F Schaefer III, and C David Sherrill, "Quadratically convergent algorithm for orbital optimization in the orbital-optimized coupled-cluster doubles method and in orbital-optimized second-order møller–plesset perturbation theory," *The Journal of Chemical Physics* **135**, 104103 (2011).
 - ¹¹ Rostam M Razban, David Stück, and Martin Head-Gordon, "Addressing first derivative discontinuities in orbital-optimized opposite-spin scaled second-order perturbation theory with regularisation," *Molecular Physics* **115**, 2102 (2017).
 - ¹² David Stück and Martin Head-Gordon, "Regularized orbital-optimized second-order perturbation theory," *The Journal of Chemical Physics* **139**, 244109 (2013).
 - ¹³ Shaama Mallikarjun Sharada, David Stück, Eric J Sundstrom, Alexis T Bell, and Martin Head-Gordon, "Wavefunction stability analysis without analytical electronic Hessians: application to orbital-optimized second-order møller–plesset theory and vv10-containing density functionals," *Molecular Physics* **113**, 1802 (2015).
 - ¹⁴ Joonho Lee and Martin Head-Gordon, "Regularized orbital-optimized second-order møller–plesset perturbation theory: A reliable fifth-order-scaling electron correlation model with orbital energy dependent regularizers," *Journal of Chemical Theory and Computation* **14**, 5203 (2018).
 - ¹⁵ Lars Goerigk and Stefan Grimme, "Double-hybrid density functionals," *Wiley Interdisciplinary Reviews: Computational Molecular Science* **4**, 576 (2014).
 - ¹⁶ Jan ML Martin and Golokesh Santra, "Empirical double-hybrid density functional theory: A "third way" in between wft and dft," *Israel Journal of Chemistry* **60**, 787 (2020).
 - ¹⁷ Simone Kossmann, Barbara Kirchner, and Frank Neese, "Performance of modern density functional theory for the prediction of hyperfine structure: meta-gga and double hybrid functionals," *Molecular Physics* **105**, 2049 (2007).
 - ¹⁸ Roberto Peverati and Martin Head-Gordon, "Orbital optimized double-hybrid density functionals," *The Journal of Chemical Physics* **139**, 024110 (2013).
 - ¹⁹ Luke W Bertels, Joonho Lee, and Martin Head-Gordon, "Polishing the gold standard: The role of orbital choice in ccSD(t) vibrational frequency prediction," *Journal of Chemical Theory and Computation* **17**, 742 (2021).
 - ²⁰ Luke W Bertels, Joonho Lee, and Martin Head-Gordon, "Third-order møller–plesset perturbation theory made useful? choice of orbitals and scaling greatly improves accuracy for thermochemistry, kinetics, and intermolecular interactions," *The journal of physical chemistry letters* **10**, 4170 (2019).
 - ²¹ Adam Rettig, Diptarka Hait, Luke W Bertels, and Martin Head-Gordon, "Third-order møller–plesset theory made more useful? the role of density functional theory orbitals," *Journal of Chemical Theory and Computation* **16**, 7473 (2020).
 - ²² Lan Nguyen Tran and Takeshi Yanai, "Correlated one-body potential from second-order møller–plesset perturbation theory: Alternative to orbital-optimized mp2 method," *The Journal of Chemical Physics* **138**, 224108 (2013).
 - ²³ Takeshi Yanai and Garnet Kin-Lic Chan, "Canonical transformation theory for multireference problems," *The Journal of Chemical Physics* **124**, 194106 (2006).
 - ²⁴ Takeshi Yanai and Garnet Kin-Lic Chan, "Canonical transformation theory from extended normal ordering," *The Journal of Chemical Physics* **127**, 104107 (2007).
 - ²⁵ Garnet Kin-Lic Chan and Takeshi Yanai, "Canonical Transformation Theory for Dynamic Correlations in Multireference Problems," in *Adv. Chem. Phys., Volume 134*, edited by D. A. Mazziotti (John Wiley & Sons, Inc., Hoboken, NJ, USA, 2007) reduced-de ed., Chap. 13, p. 343.

- ²⁶ Eric Neuscamman, Takeshi Yanai, and Garnet Kin-Lic Chan, "Quadratic canonical transformation theory and higher order density matrices," *The Journal of Chemical Physics* **130**, 124102 (2009).
- ²⁷ Eric Neuscamman, Takeshi Yanai, and Garnet Kin-Lic Chan, "Strongly contracted canonical transformation theory," *The Journal of Chemical Physics* **132**, 024106 (2010).
- ²⁸ Eric Neuscamman, Takeshi Yanai, and Garnet Kin-Lic Chan, "A review of canonical transformation theory," *International Reviews in Physical Chemistry* **29**, 231 (2010).
- ²⁹ Werner Kutzelnigg and Debashis Mukherjee, "Normal order and extended wick theorem for a multiconfiguration reference wave function," *The Journal of Chemical Physics* **107**, 432 (1997).
- ³⁰ David A Mazziotti, "Contracted schrödinger equation: Determining quantum energies and two-particle density matrices without wave functions," *Physical Review A* **57**, 4219 (1998).
- ³¹ David A Mazziotti, "Approximate solution for electron correlation through the use of schwinger probes," *Chemical Physics Letters* **289**, 419 (1998).
- ³² Werner Kutzelnigg and Debashis Mukherjee, "Cumulant expansion of the reduced density matrices," *The Journal of Chemical Physics* **110**, 2800 (1999).
- ³³ Simone Kossmann and Frank Neese, "Correlated ab initio spin densities for larger molecules: orbital-optimized spin-component-scaled mp2 method," *The Journal of Physical Chemistry A* **114**, 11768 (2010).
- ³⁴ Qiming Sun, Timothy C Berkelbach, Nick S Blunt, George H Booth, Sheng Guo, Zhendong Li, Junzi Liu, James D McClain, Elvira R Sayfutyarova, Sandeep Sharma, Sebastian Wouters, and Garnet Kin-Lic Chan, "Pyscf: the python-based simulations of chemistry framework," *Wiley Interdisciplinary Reviews: Computational Molecular Science* **8**, e1340 (2018).
- ³⁵ Werner Kutzelnigg, "Origin and meaning of the fermi contact interaction," *Theoretica Chimica Acta* **73**, 173 (1988).
- ³⁶ Martin Kaupp, Michael Buhl, and Vladimir G Malkin, *Calculation of NMR and EPR Parameters* (Wiley Online Library, 2004).
- ³⁷ Lan Nguyen Tran, Yuki Kurashige, and Takeshi Yanai, "Toward reliable prediction of hyperfine coupling constants using ab initio density matrix renormalization group method: Diatomic 2σ and vinyl radicals as test cases," *Journal of Chemical Theory and Computation* **10**, 1953 (2014).
- ³⁸ Lan Nguyen Tran, Yuki Kurashige, and Takeshi Yanai, "Scalar relativistic calculations of hyperfine coupling constants using ab initio density matrix renormalization group method in combination with third-order douglas-kroll-hess transformation: Case studies on 4d transition metals," *Journal of Chemical Theory and Computation* **11**, 73 (2015).
- ³⁹ Toru Shiozaki and Takeshi Yanai, "Hyperfine coupling constants from internally contracted multireference perturbation theory," *Journal of Chemical Theory and Computation* **12**, 4347 (2016).
- ⁴⁰ Pradipta Kumar Samanta and Andreas Köhn, "First-order properties from internally contracted multireference coupled-cluster theory with particular focus on hyperfine coupling tensors," *The Journal of Chemical Physics* **149**, 064101 (2018).
- ⁴¹ Frank Neese, Frank Wennmohs, Ute Becker, and Christoph Riplinger, "The orca quantum chemistry program package," *The Journal of Chemical Physics* **152**, 224108 (2020).
- ⁴² Frank Neese, "Prediction of electron paramagnetic resonance g values using coupled perturbed hartree-fock and kohn-sham theory," *The Journal of Chemical Physics* **115**, 11080 (2001).
- ⁴³ Lan Nguyen Tran and Eric Neuscamman, "Improving excited-state potential energy surfaces via optimal orbital shapes," *The Journal of Physical Chemistry A* **124**, 8273 (2020).
- ⁴⁴ Diptarka Hait and Martin Head-Gordon, "Orbital optimized density functional theory for electronic excited states," *The Journal of Physical Chemistry Letters* **12**, 4517 (2021).
- ⁴⁵ Jacqueline AR Shea and Eric Neuscamman, "Communication: A mean field platform for excited state quantum chemistry," *The Journal of Chemical Physics* **149**, 081101 (2018).
- ⁴⁶ Tarini S Hardikar and Eric Neuscamman, "A self-consistent field formulation of excited state mean field theory," *The Journal of Chemical Physics* **153**, 164108 (2020).
- ⁴⁷ Rachel Clune, Jacqueline AR Shea, and Eric Neuscamman, "N5-scaling excited-state-specific perturbation theory," *Journal of Chemical Theory and Computation* **16**, 6132 (2020).
- ⁴⁸ Andrew TB Gilbert, Nicholas A Besley, and Peter MW Gill, "Self-consistent field calculations of excited states using the maximum overlap method (mom)," *The Journal of Physical Chemistry A* **112**, 13164 (2008).
- ⁴⁹ Kevin Carter-Fenk and John M Herbert, "State-targeted energy projection: A simple and robust approach to orbital relaxation of non-aufbau self-consistent field solutions," *Journal of Chemical Theory and Computation* **16**, 5067 (2020).
- ⁵⁰ Shane R Yost and Martin Head-Gordon, "Size consistent formulations of the perturb-then-diagonalize møller-plesset perturbation theory correction to non-orthogonal configuration interaction," *The Journal of Chemical Physics* **145**, 054105 (2016).
- ⁵¹ Hugh GA Burton and Alex JW Thom, "Reaching full correlation through nonorthogonal configuration interaction: A second-order perturbative approach," *Journal of Chemical Theory and Computation* **16**, 5586 (2020).